Development 138, 4499-4509 (2011) doi:10.1242/dev.067454

Nephronectin regulates atrioventricular canal differentiation via Bmp4-Has2 signaling in zebrafish

Chinmoy Patra[1], Florian Diehl[1], Fulvia Ferrazzi[2,*], Machteld J. van Amerongen[1], Tatyana Novoyatleva[1], Liliana Schaefer[3], Christian Mühlfeld[4], Benno Jungblut[1] and Felix B. Engel[1,†]

SUMMARY

The extracellular matrix is crucial for organogenesis. It is a complex and dynamic component that regulates cell behavior by modulating the activity, bioavailability and presentation of growth factors to cell surface receptors. Here, we determined the role of the extracellular matrix protein Nephronectin (Npnt) in heart development using the zebrafish model system. The vertebrate heart is formed as a linear tube in which myocardium and endocardium are separated by a layer of extracellular matrix termed the cardiac jelly. During heart development, the cardiac jelly swells at the atrioventricular (AV) canal, which precedes valve formation. Here, we show that Npnt expression correlates with this process. Morpholino-mediated knockdown of Npnt prevents proper valve leaflet formation and trabeculation and results in greater than 85% lethality at 7 days post-fertilization. The earliest observed phenotype is an extended tube-like structure at the AV boundary. In addition, the expression of myocardial genes involved in cardiac valve formation (*cspg2*, *fibulin 1*, *tbx2b*, *bmp4*) is expanded and endocardial cells along the extended tube-like structure exhibit characteristics of AV cells (*has2*, *notch1b* and Alcam expression, cuboidal cell shape). Inhibition of *has2* in *npnt* morphants rescues the endocardial, but not the myocardial, expansion. By contrast, reduction of BMP signaling in *npnt* morphants reduces the ectopic expression of myocardial and endocardial AV markers. Taken together, our results identify Npnt as a novel upstream regulator of Bmp4-Has2 signaling that plays a crucial role in AV canal differentiation.

KEY WORDS: Nephronectin, Atrioventricular canal, Bmp4, Zebrafish

INTRODUCTION

The vertebrate heart is formed as a simple linear tube in which myocardium and endocardium are separated by a cell-free layer of extracellular matrix (ECM) termed the cardiac jelly. Shortly after the onset of heart looping, local differentiation pathways are activated, initiating the formation of the atrial and ventricular chambers that are separated by a discrete domain known as the atrioventricular (AV) canal. The signaling pathways that underlie these processes are highly conserved across species ranging from zebrafish to human (Stainier, 2001; Beis et al., 2005; Srivastava, 2006). However, the mechanism by which the differentiation of the AV segment in the primary heart tube is controlled remains largely unknown, although some molecular circuits of the regulatory hierarchy, such as Notch and Tbx2/Bmp2, have been implicated in previous studies.

In zebrafish, heart looping starts at ~36 hours post-fertilization (hpf). The chambers express distinct myosin genes [*vmhc*, *amhc* (*myh6* – Zebrafish Information Network) (Yelon, 2001; Berdougo et al., 2003)] whereas the expression of myocardial genes [e.g. *bmp4*, *cspg2* (*vcana* – Zebrafish Information Network) (Walsh and Stainier, 2001), *fibulin 1* (Zang et al., 1997)] and endocardial genes [e.g. *notch1b* (Walsh and Stainier, 2001), *has2* (Smith et al., 2009)] becomes restricted to the AV boundary. In addition, AV endocardial cells differentiate into cuboidal cells that express Alcam (Alcama, DM-GRASP) (Beis et al., 2005). The differentiated AV endocardial and myocardial cells produce increased amounts of ECM components resulting in cardiac jelly swelling, which initiates valve formation (Moorman and Christoffels, 2003).

Defects in cardiac valves are the most common type of congenital malformation (Loffredo, 2000). Thus, it is important to identify novel regulators of cardiac valve development. Utilizing a microarray-based temporal RNA expression data set describing heart development, we identified the gene *nephronectin* (*npnt*) as transiently expressed in the heart at the time of valve initiation and formation. Npnt has previously been identified as a ligand of integrin α8β1 (Brandenberger et al., 2001; Sato et al., 2009). It contains an N-terminal signal peptide followed by EGF-like repeats, an RGD sequence and a C-terminal MAM domain, but it does not contain a transmembrane domain. Thus, Npnt has been classified as an ECM protein (Brandenberger et al., 2001). Recent data have shown that Npnt is required for the invasion of the metanephric mesenchyme by the ureteric bud during kidney development (Linton et al., 2007). Furthermore, it has been associated with malignant melanoma. Npnt overexpression in melanoma cell lines increased cell adhesion and decreased cell migration (Kuphal et al., 2008). In addition, overexpression of Npnt in mouse MC3T3-E1 cells promoted their differentiation into osteoblasts, an effect mediated via the EGF-like repeats (Fang et al., 2010; Kahai et al., 2010). However, to our knowledge, Npnt expression has not thus far been associated with heart development and its function remains poorly characterized.

[1]Department of Cardiac Development and Remodelling, Max-Planck-Institute for Heart and Lung Research, Parkstrasse 1, 61231 Bad Nauheim, Germany. [2]Dipartimento di Informatica e Sistemistica, Università degli Studi di Pavia, via Ferrata 1, 27100 Pavia, Italy. [3]Institute for General Pharmacology and Toxicology, Goethe University, Theodor-Stern Kai 7, 60590 Frankfurt/Main, Germany. [4]Institute of Anatomy and Cell Biology, Justus-Liebig-University Giessen, Aulweg 123, 35385 Giessen, Germany.

*Present address: Gene Center, Ludwig-Maximilians-Universität München, Feodor-Lynen-Str. 25, 81377 Munich, Germany
†Author for correspondence (felix.engel@mpi-bn.mpg.de)

Accepted 9 August 2011

Here, we identify Npnt as a novel regulator of heart development. Our data show that Npnt is an upstream regulator of Bmp4-Has2 signaling and that it is critically involved in AV canal differentiation during zebrafish heart development.

MATERIALS AND METHODS

Zebrafish maintenance

Wild-type AB and transgenic *Tg(myl7:EGFP-HsHRAS)*^{s883} (D'Amico et al., 2007), *Tg(kdrl:EGFP)*^{s843} (Jin et al., 2005), *Tg(–5.1myl7:nDsRed2)f2* (Mably et al., 2003) and *Tg(TOP:GFP)*^{w25} (Dorsky et al., 2002) zebrafish (*Danio rerio*) were maintained at 28°C as described (Westerfield, 1993).

Microarray data

Total RNA of rat cardiac ventricles from different developmental stages [embryonic day (E) 11 to postnatal day (P) 10.5] at 12-hour intervals was isolated using Trizol (Invitrogen). For each time point, the RNA was extracted from 6-122 pooled hearts after removal of the atria. In addition, three independent RNA samples were generated for E11, E15, E19 and P2. Expression analysis was performed using the Affymetrix GeneChip RAT 230 Expression Set. Preprocessing of the data, i.e. background subtraction, normalization and probeset summarization, were performed according to the robust multi-array average (RMA) procedure.

Reverse transcriptase PCR (RT-PCR)

RNA was extracted from 30 or more zebrafish embryos at the indicated developmental stages, adult zebrafish tail fin or rat heart ventricles (E11 to E20, $n \geq 10$; P5, P10 and adult, $n \geq 3$) using Trizol (Invitrogen). RT-PCR was performed following standard protocols. Primers (5′ to 3′) for rat were: *Gapdh*, CAGAAGACTGTGGATGGCCC and AGTGTAGCCCAGGATGCCCT; *Npnt* total, CACAGTGCAAACACGGAGAG and GCATCAGCATGTATCCGTTG; *Npnt* variants, CTGGGGACAGTGTCAACCTT and GCATCAGCATGTATCCGTTG. Primers for zebrafish were: *gapdh*, TGGGTGTCAACCATGAGAAA and AACCTGGTGCTCCGTGTATC; *npnt* F1, CATTCGGGAGCTTCAAGTGT; F2, ATGTGGATCATAAAGTTCATGTTGA; F3, CAATGGTCTGTGTCGGTACG; R, CTGAAGGTCAAAGCCGTCAT; R2, TGTCATTATGGGGTATTGTGTGA; and R3, TCATCCTACCGCACTCTGTTG.

In situ hybridization

At 24 hpf, 0.2 mM 1-phenyl-2-thiourea was used to prevent pigmentation. Embryos were fixed in 4% paraformaldehyde (PFA) in PBS for 2 hours at room temperature (RT), washed twice (0.1% Tween 20 in PBS, 4°C), dehydrated and processed for in situ hybridization utilizing digoxigenin-labeled RNA probes against: *vmhc* (Yelon, 2001), *amhc* (Berdougo et al., 2003), *cspg2*, *notch1b*, *bmp4* (Walsh and Stainier, 2001), *fibulin 1* (Zang et al., 1997), *tbx2b* (Smith et al., 2009), *has2* (Bakkers et al., 2004), *gfp*, *npnt* and *zgc:172265* (NM_001114911.1), which is named in this study *itga8* owing to its homology to *itga8* of other species (UniGene Cluster UGID:2630752) (see Fig. S9 in the supplementary material). For in situ probes against *npnt* and *itga8* mRNA, 517 bp (*npnt*, 5′-CAATGGTCTGTGTCGGTACG-3′ and 5′-CTGAAGGTCAAAGCCGTCAT-3′) and 713 bp (*itga8*, 5′-GAAAAGCCCACGGTTTACAA-3′ and 5′-TCCCCTGTGAACTCTCCAAC-3′) fragments were amplified from cDNA and cloned into the pGEM-T Easy vector (Promega) to create pGEMTeasy-Z*npnt* and pGEMTeasy-*itga8*. Whole-mount embedded embryos (17% gelatine in PBS) were fixed with 4% PFA in PBS (overnight at RT), sectioned (120 μm) and mounted (Kaiser's glycerol gelatin, Merck). For thin sections (Leica RM2255), embryos were embedded in paraffin (*npnt*, 4 μm) or epoxy resin (*bmp4*, 2 μm).

Cloning of zebrafish *npnt* and microinjection

A 1945 bp fragment of zebrafish *npnt* cDNA (NM_001145580) was amplified with TopTaq DNA polymerase (Qiagen) using RNA derived from 52 hpf embryos and primers 5′-CACCATGTGGATCATAAAGTTCATGTTGA-3′ and 5′-TCATCCTACCGCACTCTGTTG-3′, purified, cloned (pGEM-T Easy), subcloned into pCS2+ after *Eco*RI digestion (pCS2+-F*npnt*) and sequenced. Capped *npnt* mRNA was generated after linearization (pCS2+-F*npnt*, *Sac*II) using the mMESSAGE mMACHINE SP6 In Vitro Transcription Kit (Ambion). One-cell stage embryos were injected into the yolk (≤4 nl; PV820 Injector, World Precision Instruments) with morpholinos (*npnt* MO1, 5′-CATGAACTTTATGATCCACATCTCC-3′; *npnt* MO2, 5′-TGTGAAACGGCAGACGGAACTCACT-3′; *npnt* MO3, 5′-GAATAGGCTAAGTGCCGTCTCACCT-3′; *has2* MO, 5′-AGCAGCTCTTTGGAGATGTCCCGTT-3′; Gene Tools) and/or capped *npnt* mRNA in 0.1 M KCl. Control injection was with 0.05% Phenol Red (Sigma).

Wnt signaling and BMP signaling inhibition

Wnt signaling inhibition was achieved by overexpressing Dkk1 using *Tg(hsp70l:dkk1-GFP)*^{w32}. MO2- or control-injected *Tg(hsp70l:dkk1-GFP)*^{w32} embryos were raised at 28°C and heat shocked at 37°C for 30 minutes at 36 hpf or 40 hpf. Cardiac morphology was analyzed at 52 hpf using bright-field microscopy. Dorsomorphin (Tocris) dissolved in water was used to inhibit BMP signaling (Yu et al., 2008) and was added at 10 μm at 25 hpf in E3 medium.

Western blot

Protein was isolated from 60 embryos at 2 days post-fertilization (dpf). Yolk was removed by shearing (pipetting), shaking twice for 3 minutes each at 1100 rpm in deyolking buffer (55 mM NaCl, 1.8 mM KCl, 1.25 mM $NaHCO_3$) and washing in 110 mM NaCl, 3.5 mM KCl, 2.7 mM $CaCl_2$, 10 mM Tris-HCl (pH 8.5). Embryos were pelleted (300 ***g***, 1 minute, 4°C) and lysed by sonication (four pulses of 5 seconds each) in lysis buffer [Cell Signaling buffer plus protease inhibitor mix (Roche) and 1 mM PMSF (Sigma)]. After centrifugation (17,000 ***g***, 5 minutes, 4°C) supernatants were resolved in NuPAGE Novex Bis-Tris Gels (Invitrogen), blotted and analyzed with anti-Npnt (1:300, Cosmo Bio), anti-p-Smad1/5/8 (1:1000, Cell Signaling), anti-acetylated tubulin (1:1000, Sigma) or anti-pan-Actin (Cell Signaling, 1:1000) antibody.

Immunohistochemistry and histological analysis

Immunohistochemistry was performed as described (Dong et al., 2007). Samples were incubated with anti-Alcam (zn8) (1:10, DSHB) or s46 (1:10, DSHB) antibody, DsRed antibody (1:200, Clontech) and subsequently labeled with Alexa-conjugated secondary antibodies (Molecular Probes). Staining with anti-p-Smad1/5/8 antibody (1:200, Cell Signaling) was performed with minor modifications: fixation in 2% PFA in PBS for 1.5 hours at RT; blocking in 10% goat serum/0.3% Triton X-100 in PBS. For F-actin staining, samples were incubated with Rhodamine-labeled phalloidin (1:75, Invitrogen) for 1 hour at RT in PBDT (0.1% DMSO, 0.1% Triton X-100 in PBS). For localization of hyaluronan, 4 μm paraffin sections were treated with 3% H_2O_2 for 10 minutes at RT and then incubated with biotinylated HA-binding protein (bHABP, Calbiochem, 5 μg/ml, diluted in 50 mM Tris, 150 mM NaCl, pH 7.4) at 4°C overnight. After washing, sections were incubated with HRP-conjugated avidin followed by incubation with 3,3′-diaminobenzidine peroxidase substrate (Vector Laboratories) and counterstaining with Hematoxylin (AppliChem). The specificity of staining was tested by treating sections with 100 U hyaluronidase (Sigma) for 30 minutes at 37°C prior to incubation with bHABP.

Morphological analysis, confocal and transmission electron microscopy (TEM)

For Nomarski (Zeiss) and confocal microscopy, tricane-anesthetized embryos were mounted in 1% low-melting-point agarose in E3 medium. Confocal sections (1.3 μm) covering the entire heart were imaged on a Zeiss LSM710 and images were processed to obtain projections (LSM Image Browser, Zeiss). For TEM, embryos were fixed by immersion in 1.5% glutaraldehyde/1.5% paraformaldehyde in 0.15 M HEPES buffer (pH 7.3) for at least 24 hours. The specimens were subsequently osmicated, stained en bloc with uranyl acetate, dehydrated in an ascending ethanol series and embedded in epoxy resin. Ultrathin sections from comparable regions of the heart were generated and analyzed using a Zeiss TEM 902.

Live imaging

Movies of embryos embedded in 1% low-melting-point agarose in E3 medium under a Leica DM6000 B microscope were recorded with a Sony HDR-SR12 camcorder and formatted (Wondershare or iSkysoft video converter).

Statistical analysis

Data are expressed as the mean ± s.e.m. of at least three independent experiments. Statistical significance of differences was evaluated by one-way ANOVA followed by Bonferroni's post-hoc test (GraphPad Prism). $P<0.05$ was considered statistically significant.

RESULTS

npnt is transiently expressed during heart development

Based on a large-scale temporal RNA expression analysis we have identified nephronectin (*Npnt*) as transiently expressed in the rat heart at the time of valve initiation and formation (Fig. 1A) (Okagawa et al., 1996). These results were confirmed by RT-PCR for both known variants of rat *Npnt* using independent sets of mRNA (Fig. 1B). To determine the expression pattern of *npnt* in zebrafish, we performed whole-mount in situ hybridization analyses. At 24 hpf, *npnt* is markedly expressed at the tail bud, head, in the posterior part of the gut and in the pharyngeal endoderm (Fig. 1C,D). At 34 hpf, highest expression was observed in the pronephric region, with persistent expression in the head (Fig. 1E,F). *npnt* expression in the heart was first detected at 44 hpf (Fig. 1G,H). Thin sections demonstrated that *npnt* is expressed in the myocardium throughout the heart (Fig. 1I,J). Cardiac *npnt* expression was still observed at 48 hpf, but was undetectable at 53 hpf when *npnt* expression was most prominent in the pharynx, esophagus and the pharyngeal endoderm (Fig. 1K,L). Taken together, our data demonstrate that *npnt* is transiently expressed during heart development.

Npnt knockdown disrupts heart development and is lethal

To assess the role of Npnt in zebrafish heart development we applied antisense morpholino oligonucleotides. We designed one translation-inhibitory morpholino (MO1) and two splicing-inhibitory morpholinos that target the splice donor site of exon E5 (MO2) or exon E1 (MO3) (Fig. 2A, see Fig. S1A in the supplementary material). Our data indicate that both MO2 and MO3 were effective in disrupting correct splicing of *npnt* pre-mRNA, resulting in a marked decrease of mature *npnt* mRNA (Fig. 2B,C, see Fig. S1B in the supplementary material). RT-PCR analyses demonstrated that MO2 injection resulted in intron insertion (Fig. 2B) and exon E5 deletion, which was confirmed by sequencing (Fig. 2C). Western blot analysis demonstrated that injection of MO1 (3.5 pmol), MO2 (1.4 pmol) and MO3 (2.4 pmol) resulted in a marked decrease in the Npnt protein level (Fig. 2D, see Fig. S1C in the supplementary material). Therefore, all subsequent studies were performed using these amounts of morpholinos. Collectively, our results demonstrate that injection of MO1, MO2 and MO3 efficiently knocked down the expression of Npnt on the mRNA and/or protein level.

To determine the effect of Npnt knockdown on heart development we injected morpholinos into the embryos of *Tg(myl7:EGFP-HsHRAS)*^{s883} transgenic zebrafish ($n>200$, four independent experiments), in which GFP is localized at the cardiomyocyte plasma membrane, facilitating live imaging of heart morphology. MO1, MO2 or MO3 injection did not show any obvious effect on zebrafish development until 40 hpf. However, Npnt knockdown resulted in 89±7.9% (mean ± s.e.m.) lethality at

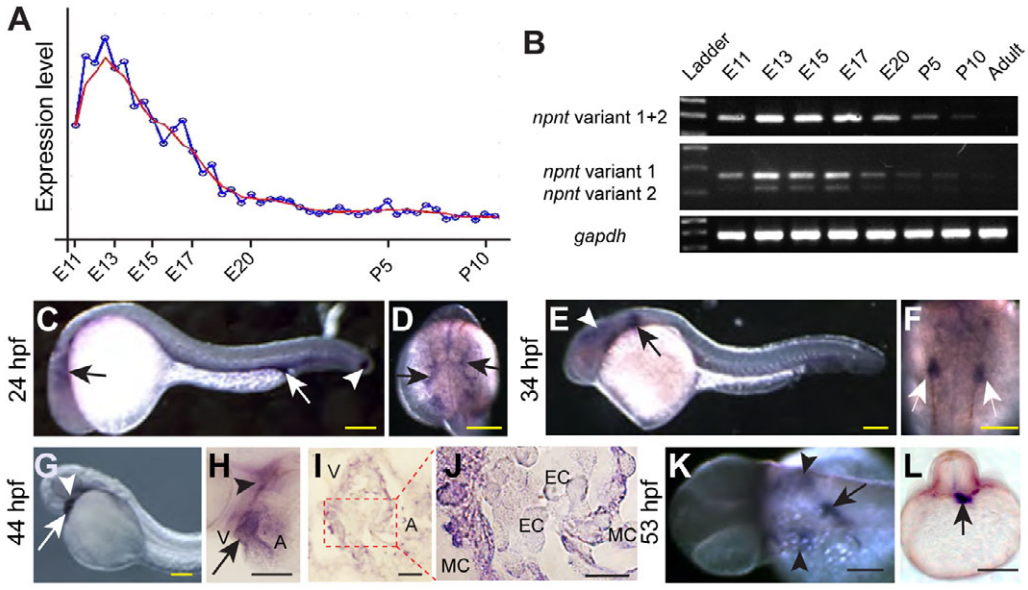

Fig. 1. *npnt* is transiently expressed during rat and zebrafish heart development. (**A**) *Npnt* expression levels in rat heart tissue from E11 to P10.5 in 12-hour intervals according to microarray analysis (Affymetrix GeneChip Rat Expression Set 230). Blue line, real profile; red line, smoothened profile. (**B**) RT-PCR analysis of *Npnt* mRNA expression during rat heart development. *Gapdh* was used as loading control. Ladder indicates a size marker. (**C-L**) Zebrafish *npnt* expression determined by whole-mount in situ hybridization. (C) Lateral view of a 24 hpf embryo showing *npnt* expression at tailbud (white arrowhead), head (black arrow) and posterior part of the gut (white arrow). (D) Dorsal view of the anterior part of the trunk demonstrating expression in pharyngeal endoderm (arrows). (E,F) Lateral (E) and dorsal (F) views at 34 hpf showing expression in the pronephric region (arrows) and head (arrowhead). (G,H) Ventrolateral view (G) and parasagittal section (H) at 44 hpf demonstrating *npnt* expression in heart (arrows) and jaw (arrowheads). (I,J) Paraffin section (4 μm) confirming expression in the myocardium (I, 200×; J, 1000×). (K) Dorsal view showing *npnt* expression at 53 hpf in pharynx, esophagus (arrow) and pharyngeal endoderm (arrowheads). (L) Transverse section through the trunk confirming expression in the endodermal cells of the anterior gut (arrow). A, atrium; EC, endocardium; MC, myocardium; V, ventricle. Scale bars: 100 μm in C-H,K,L; 50 μm in I; 20 μm in J.

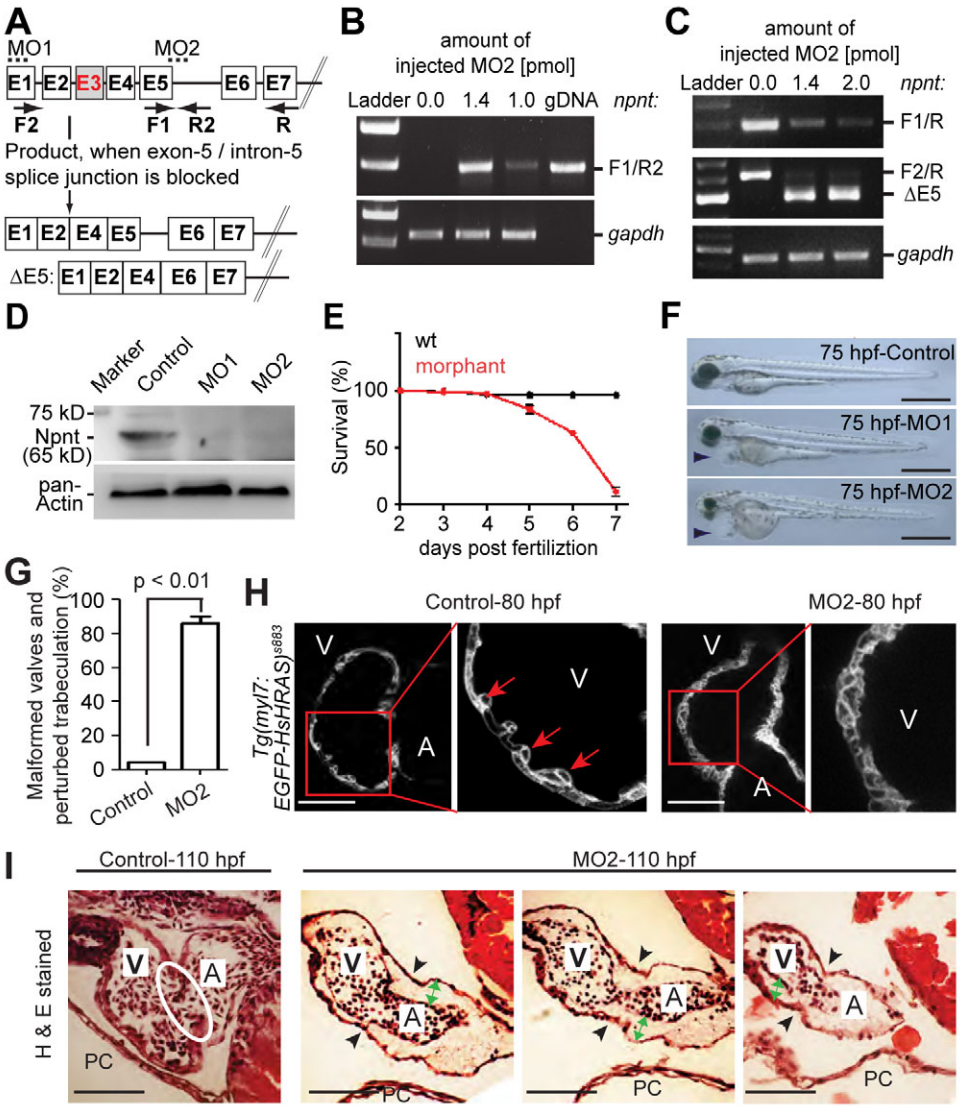

Fig. 2. Npnt knockdown disrupts heart development and is lethal. (**A**) Scheme of the effect of *npnt* splice-inhibitory morpholino MO2. Exons are represented by boxes and introns by lines. Dotted lines indicate the region targeted by MO1 or MO2 and arrows indicate RT-PCR primer positions. Exon E3 could not be detected. (**B**,**C**) RT-PCR analysis of mRNAs from control and MO2-injected zebrafish embryos at 52 hpf using *npnt* primers as indicated in A and *gapdh* primers (loading control) (*n*=3). MO2 inhibited *npnt* pre-mRNA splicing, resulting in intron insertion (B) and exon E5 deletion (C). (**D**) Western blot analysis of control and MO1- or MO2-injected embryos at 52 hpf (*n*=3). Both morpholinos efficiently knocked down the Npnt protein level. (**E**) Npnt knockdown resulted in 89±7.9% (mean ± s.e.m.) lethality at 7 dpf. (**F**) Lateral view of control, MO1- or MO2-injected embryos at 75 hpf. MO1 or MO2 injection resulted in pericardial edema (arrowheads). (**G**) Quantitative analysis. Valve formation and trabeculation are perturbed in 86±3.9% (mean ± s.e.m.) of morphant hearts at 110 hpf. (**H**) Confocal images of hearts from control and MO2-injected embryos from transgenic *Tg(myl7:EGFP-HsHRAS)*^{s883} zebrafish at 80 hpf suggesting that the initiation of trabeculation is perturbed in *npnt* morphants. Red arrows indicate trabeculae. (**I**) Hematoxylin and Eosin (H&E)-stained sagittal sections of hearts from control and MO2-injected embryos at 110 hpf. In contrast to morphants, control embryos develop proper atrioventricular (AV) valve leaflets (white oval). Black arrowheads indicate the AV boundary; green arrows indicate expanded cardiac jelly. A, atrium; V, ventricle; PC, pericardium. Scale bars: 500 μm in F; 50 μm in H,I.

7 dpf (Fig. 2E). The first obvious phenotype was pericardial edema at 75 hpf, indicating a cardiac defect (Fig. 2F, see Fig. S1D in the supplementary material). A closer analysis of morphant hearts revealed that valve formation and trabeculation at 110 hpf were perturbed in 86±3.9%, with more than 30% of those lacking of valve leaflets as well as trabeculation (Fig. 2G-I). The morphants are also characterized by cardiac jelly swelling throughout the heart (Fig. 2I). Live imaging revealed no obvious differences between wild type and morphants in cardiac function and circulation at 36 hpf and 52 hpf (see Movies 1-4 in the supplementary material). Taken together, our data indicate that *npnt* is essential for cardiac development in zebrafish.

npnt morphant hearts have an extended AV canal

To determine the earliest heart phenotype we utilized transgenic zebrafish lines *Tg(myl7:EGFP-HsHRAS)*^{s883} and *Tg(–5.1myl7:nDsRed2)f2*, which express RFP in cardiomyocyte nuclei. Npnt depletion induced formation of an extended tube-like

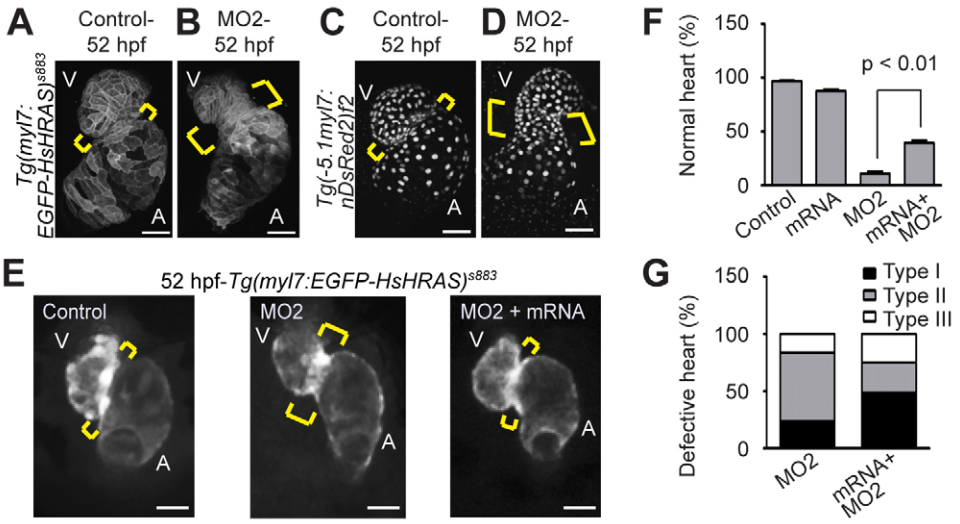

Fig. 3. Npnt knockdown causes extension of the AV canal. (**A-D**) Projections of confocal images of hearts from control (A,C) and MO2-injected (B,D) embryos from transgenic *Tg(myl7:EGFP-HsHRAS)*^{s883} (A,B) and *Tg(–5.1myl7:nDsRed2)f2* (C,D) zebrafish at 52 hpf, suggesting an extension of the AV canal (brackets) in *npnt* morphants. (**E**) Representative images of hearts from control, MO2-injected and MO2 + *npnt* mRNA-injected embryos from transgenic *Tg(myl7:EGFP-HsHRAS)*^{s883} zebrafish at 52 hpf. Brackets indicate the AV boundary. (**F**) Quantitative analysis (*n*>160 from three independent experiments; mean ± s.e.m.). Note that injection of *npnt* mRNA rescued the MO2-mediated AV canal extension. (**G**) Quantitative analysis scoring of type I (mild extension of the AV canal), type II (obvious extension of the AV canal) and type III (straight heart) AV canal defects (mean ± s.e.m.). A, atrium; V, ventricle. Scale bars: 50 μm.

structure at the AV boundary at 52 hpf, as compared with control hearts from non-injected or Phenol Red-injected embryos (*n*>200, four independent experiments) (Fig. 3A-D, see Fig. S1E in the supplementary material). Based on the severity of the cardiac defect at 52 hpf, morphants were categorized into three classes: type I, mild AV canal extension; type II, obvious AV canal extension; type III, straight heart (see Fig. S2A in the supplementary material). MO1 injection caused heart defects in 71±4.0% of embryos (type I, 29±2.6%; type II, 54±5.3%; type III, 17±8.3%) and MO2 injection in 86±4.4% of embryos (type I, 21±3.2%; type II, 56±4.0%; type III, 23±3.9%) (see Fig. S2B,C in the supplementary material). All three morpholinos resulted in Npnt knockdown and in similar phenotypes, suggesting that the observed phenotypes are a functional consequence of Npnt depletion.

To prove that the observed AV canal phenotype is specific to Npnt depletion we performed rescue experiments by co-injecting capped *npnt* mRNA and MO2. Note that MO2, as a splice-inhibitory morpholino, does not affect the translation of injected *npnt* mRNA. Sequencing indicated that all cloned *npnt* cDNAs lacked exon E3 (51 bp) and a part of exon E13 and contained an additional exon E14, as compared with the *npnt* sequence published by NCBI (see Fig. S3 in the supplementary material). RT-PCR analyses of cDNA derived from zebrafish embryos at different developmental stages confirmed that this is the major splice variant (see Fig. S4A,B in the supplementary material). In adult zebrafish tail fin tissue only, we detected a second variant (see Fig. S4B in the supplementary material). Sequencing analysis demonstrated that this variant contains exon E3 but lacks part of exon E13. A Motif Scan analysis revealed no change in the overall domain structure of the proteins encoded by the two variants (see Fig. S4C,D in the supplementary material).

Assuming that the cloned cDNA represents the *npnt* mRNA at 52 hpf, we used linearized pCS2+-F*npnt* plasmid as template to generate capped *npnt* mRNA. Injection of 50 pg capped *npnt* mRNA rescued the AV extension in a subset of MO2-injected embryos (Fig. 3E,F) and had only a minor effect on cardiac development when injected alone (88±1.5% normal hearts; Fig. 3F). Importantly, 40±2.3% of embryos had normal hearts after co-injection of *npnt* mRNA and MO2 as compared with 11±2.0% after MO2 injection alone (Fig. 3F). In addition, injection of 50 pg capped *npnt* mRNA markedly reduced the severity of the AV canal defect in the remaining embryos, with defective hearts showing an increase in type I defects (from 23.6±1.2% to 48.7±2.4%) and a decrease in type II defects (from 60±1.1% to 26.5±2.6%) (Fig. 3G). The slight increase in the type III phenotype (from 16.4±2.4% to 24.8±2.4%) might be due to *npnt* overexpression. In summary, the rescue experiments confirm that the MO-mediated phenotypes are due to Npnt depletion.

To characterize the extended tube-like structure at the AV boundary we performed Alcam staining of embryos from the transgenic zebrafish line *Tg(kdrl:EGFP)*^{s843}, in which GFP is expressed in all endothelial cells. At 52 hpf, all cardiomyocytes and endocardial cells at the AV boundary express Alcam. The AV canal in wild-type animals is 5-6 tiers long at the superior AV boundary (SAV) and 3-4 tiers long at the inferior AV boundary (IAV) of Alcam-positive endocardial cells (Fig. 4A). In *npnt* morphants, the AV canal was extended by 84.4±27.6% (8-12 tiers, SAV) or 85.0±22.5% (5-7 tiers, IAV) (Fig. 4B,C). In accordance with these data, endocardial expression of *notch1b* was also expanded in *npnt* morphant hearts at the AV boundary as compared with control hearts (Fig. 4D). These data suggest that Npnt knockdown causes an increase in the number of AV endocardial cells and thus an expansion of endocardial AV specification.

In contrast to the AV endocardium, there is no AV myocardium-specific marker available. Therefore, we used genes as markers whose expression becomes restricted during development to the AV myocardium: *cspg2* (Versican), *fibulin 1* and *bmp4* (Zang et al., 1997; Walsh and Stainier, 2001); *bmp4* is also expressed at the outflow and inflow tract (Fig. 4E-G) (Walsh and Stainier, 2001). Compared with control hearts, expression of *cspg2*, *fibulin 1* and

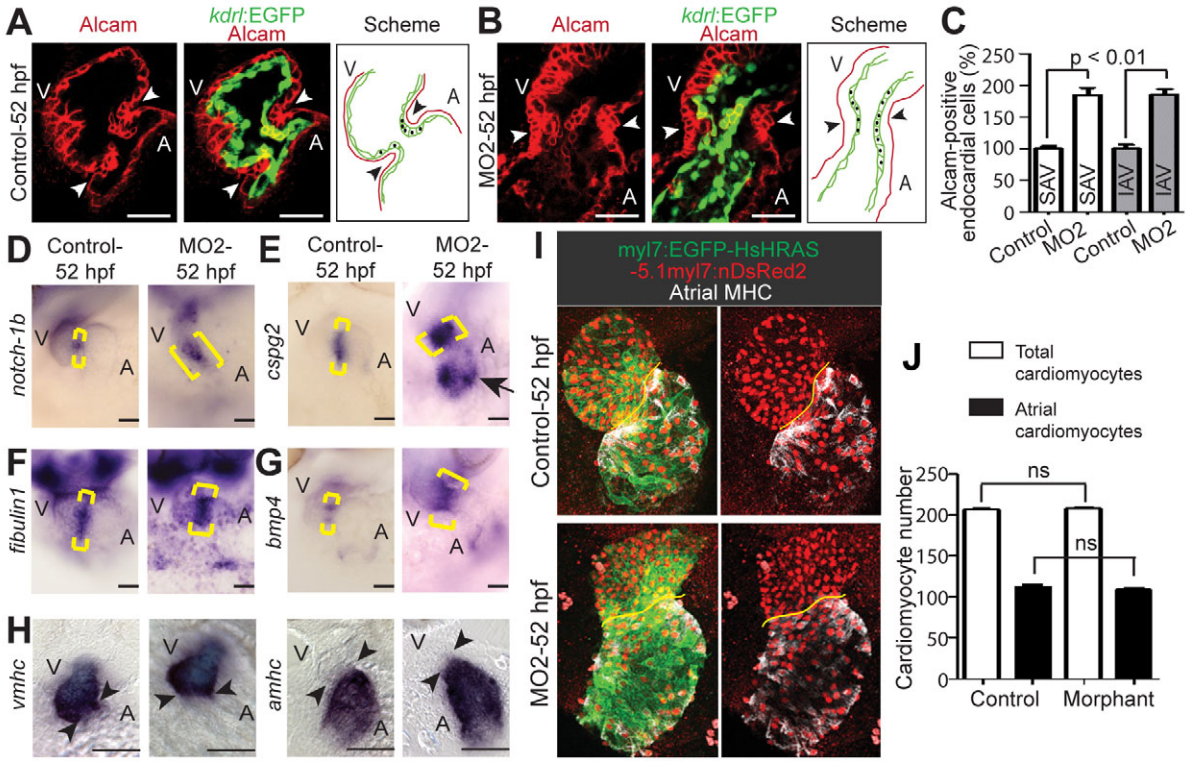

Fig. 4. Characterization of the extended AV canal. (**A**,**B**) Confocal sections of whole-mount Alcam-stained (red, indicating myocardium and differentiated endocardial cells) control (A) and MO2-injected (B) embryos from transgenic *Tg(kdrl:EGFP)*^{s843} zebrafish at 52 hpf. Npnt depletion caused an increase in differentiated endocardial cells (cuboidal in shape, Alcam positive and EGFP positive) at the AV boundary. Arrowheads indicate the AV boundary; red line, myocardium; green, endocardial cells; black dots, Alcam-positive endocardial cells. (**C**) Quantitative analysis of Alcam-positive endocardial cells (mean ± s.e.m.). SAV, superior AV; IAV, inferior AV. (**D-G**) Sections of 52 hpf control and MO2-injected embryos after whole-mount in situ hybridization for *notch1b* (D), *cspg2* (E), *fibulin 1* (F) and *bmp4* (G). Expression of these genes was expanded in *npnt* morphants (brackets). (**H**) In situ hybridization with probes against the chamber-specific marker genes *amhc* and *vmhc*. (**I**) Projections of confocal images of hearts from whole-mount control and MO2-injected embryos from double-transgenic [*Tg(–5.1myl7:nDsRed2)f2* × *Tg(myl7:EGFP-HsHRAS)*^{s883}] zebrafish stained for atrial myosin heavy chain (MHC, white) and DsRed (red). Yellow line, AV junction. (**J**) Quantitative analysis of total (chambers + AV boundary) and atrial cardiomyocyte number (mean ± s.e.m.). ns, not significant. A, atrium; V, ventricle. Scale bars: 50 μm.

bmp4 was expanded in *npnt* morphant hearts at 52 hpf (Fig. 4E-G). In addition, ectopic expression of *cspg2* was detected at the inflow tract (Fig. 4E). By contrast, chamber-specific expression of the cardiac marker genes *vmhc* and *amhc* (Yelon et al., 1999) appeared normal (Fig. 4H). Our data suggest that the extended tube-like structure represents, on a molecular level, an extended AV canal. However, owing to the lack of an AV myocardium-specific marker it remains unclear whether Npnt regulates myocardial in addition to endocardial AV specification.

To determine the origin of the additional myocardial AV canal-like cells we performed cell count experiments with double-transgenic animals [*Tg(–5.1myl7:nDsRed2)f2* × *Tg(myl7:EGFP-HsHRAS)*^{s883}]. The overall number of cardiomyocytes (chambers + AV boundary) was not significantly different between control and morphant hearts (Fig. 4I,J). These data support the assumption that the AV boundary extension is not due to an increase in cardiomyocyte number, but rather to differentiation into AV canal-like cells at the expense of chamber cells.

Npnt knockdown causes cardiac jelly expansion and increases *has2* expression

One characteristic of AV cells is increased expression of ECM components at the onset of looping. Signaling between myocardium and endocardium is essential for heart development, including valve formation (Armstrong and Bischoff, 2004; Hsieh et al., 2006; Holtzman et al., 2007). In addition, it has been suggested that an increase in cardiac jelly can interfere with this signaling and perturb heart development (Shirai et al., 2009). To determine whether the extended AV canal produces normal amounts of cardiac jelly we used *Tg(kdrl:EGFP)*^{s843} embryos, counterstained with Rhodamine-phalloidin (which detects F-actin) to visualize the myocardium. Analysis of confocal sections of hearts from control and *npnt* morphant hearts at 52 hpf showed that the space between endocardium and myocardium is markedly increased in morphants (Fig. 5A,B), suggesting that Npnt knockdown causes cardiac jelly expansion.

A major constituent of cardiac jelly is glycosaminoglycan hyaluronan (HA), which is synthesized by the product of *hyaluronan synthase 2* (*has2*), a downstream target of Tbx2 (Shirai et al., 2009). Both *has2* and *tbx2* are regulated by BMP signaling (Camenisch et al., 2000; Gaussin et al., 2002; Shirai et al., 2009). In wild-type zebrafish, the expression of both genes is restricted to the AV boundary at 2 dpf (Walsh and Stainier, 2001; Hurlstone et al., 2003; Chi et al., 2008) (Fig. 5C,E). By contrast, expression of *has2* and *tbx2b* was expanded in *npnt* morphants (Fig. 5D,F). Importantly, our data demonstrate that the phenotype was also rescued on a molecular (*bmp4*, *cspg2*) and cellular (Alcam) (see Fig. S5 in the supplementary material) level in morphologically rescued *npnt* morphants.

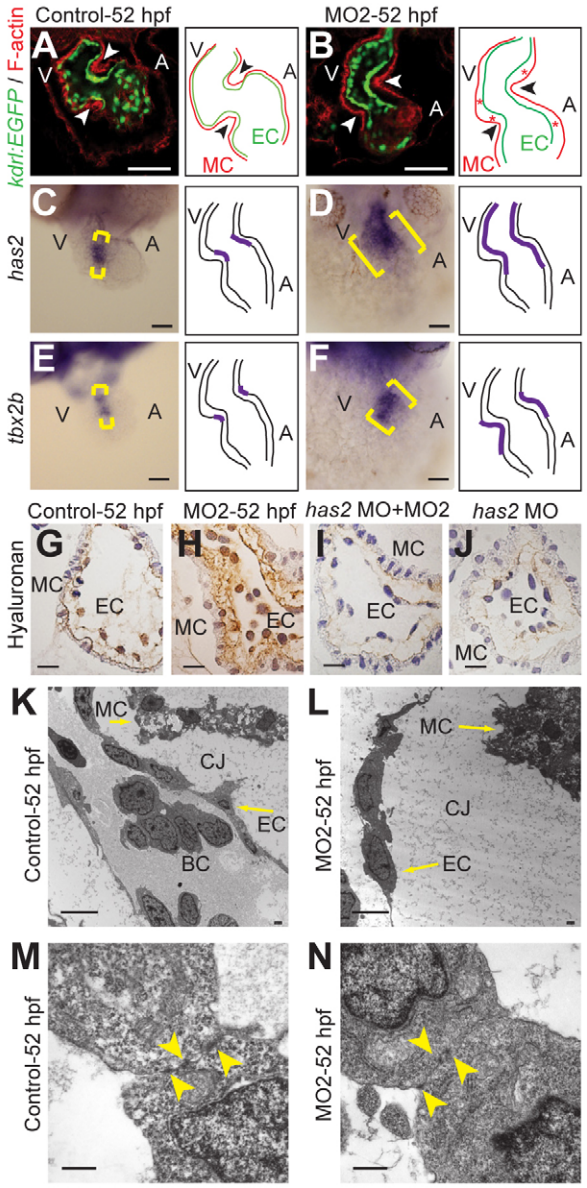

Fig. 5. Npnt knockdown causes cardiac jelly expansion and expanded expression of *has2* and *tbx2b*. (**A**,**B**) Confocal sections from whole-mount F-actin-stained (red) control (A) and MO2-injected (B) *Tg(kdrl:EGFP)*^{s843} zebrafish embryos at 52 hpf. The space between endocardium and myocardium was increased at the AV boundary (arrowheads) and throughout the chambers (red asterisks) in *npnt* morphants. (**C-F**) Sections of 52 hpf control and MO2-injected embryos after whole-mount in situ hybridization for *has2* and *tbx2b* expression (brackets). Note that the expression of these genes is expanded in *npnt* morphants. (**G-J**) Sections (4 μm) of control, MO2-, *has2* MO-, or *has2* MO + MO2-injected zebrafish embryos at 52 hpf stained for hyaluronan (brown) and counterstained with Hematoxylin (blue). (**K-N**) Transmission electron microscopy of hearts (K,L) and endocardial cells (M,N) from control and MO2-injected embryos at 52 hpf. Arrowheads indicate junctional complexes. A, atrium; BC, blood cell; CJ, cardiac jelly; EC, endocardium; MC, myocardium; V, ventricle. Scale bars: 50 μm in A-F; 10 μm in G-J; 5 μm in K,L; 1 μm in M,N.

To investigate the cause of cardiac jelly expansion we performed HA staining and transmission electron microscopy (TEM) analyses. The specificity of HA staining was tested using hyaluronidase (see Fig. S6 in the supplementary material). Npnt knockdown increased the amount of HA in the cardiac jelly compared with wild-type embryos (Fig. 5G,H). Has2 knockdown caused a marked reduction of HA in the cardiac jelly, both in *npnt* morphants (Fig. 5I) and in wild-type embryos (Fig. 5J). In addition, TEM analyses revealed that the density of cardiac jelly in wild type and *npnt* morphants is comparable (Fig. 5K,L) and that the junctional complexes (comprising adherens and tight junctions) in the endocardium in *npnt* morphants are still intact, suggesting that the expanded cardiac jelly is not due to increased permeability of the endocardium (Fig. 5M,N). These results show that Npnt is an inhibitory upstream regulator of *bmp4*, *tbx2b* and *has2* expression and thus regulates the composition of the cardiac jelly. At 40 hpf, before *npnt* expression, *bmp4* expression was restricted to the AV canal in both wild-type embryos and *npnt* morphants (see Fig. S7A in the supplementary material). This indicates that Npnt is required to maintain the restricted expression of AV canal markers.

Has2 knockdown rescues the *npnt* morphant endocardial phenotype

has2 plays an essential role during valve formation (Camenisch et al., 2000). An effect on the number of AV canal cells has not been reported. To determine whether expanded expression of *has2* caused the increased number of AV endocardial cells we performed Has2 knockdown experiments. One-cell stage embryos were injected with *has2* and *npnt* morpholinos and analyzed for AV endocardial (Alcam and *notch1b*) and myocardial (*cspg2*, *bmp4*) specific gene expression at 52 hpf (Fig. 6). Has2 knockdown in *npnt* morphants reduced the number of Alcam-positive AV endocardial cells from 180.8±21.9% (8-11 tiers, SAV) or 188.2±33.5% (5-8 tiers, IAV) to 30.8±10.5% (1-2 tiers, SAV) or 11.0±16.1% (0-1 tier, IAV) compared with wild-type embryos (Fig. 6A,B). Has2 knockdown in wild-type embryos resulted in a reduction from 100±8.6% (5-6 tiers, SAV) or 100±16.1% (3-4 tiers, IAV) to 25.1±16.1% (0-2 tiers, SAV) or 5.9±13.2% (0-1 tier, IAV) (Fig. 6A,B). In addition, Has2 knockdown rescued the expansion of *notch1b* (Fig. 6C). These data demonstrate that *has2* is required for prevalvular endocardial cell differentiation. Taken together, our data show that the increased number of AV endocardial cells in *npnt* morphants is due to the expanded expression of *has2*.

To assess whether expanded expression of *has2* caused the myocardial phenotype, we determined the expression of *cspg2* and *bmp4* after Has2 knockdown in control and *npnt* morphant embryos. The expression of these genes in *npnt* morphants as well as in control embryos either remained unchanged or was upregulated after Has2 knockdown (Fig. 6C). These data indicate that ectopic endocardial cell differentiation, but not the myocardial phenotype, in *npnt* morphants is due to ectopic expression of *has2*.

Inhibition of BMP signaling reduces AV canal expansion

Bmp4 is a major regulator for cardiac valve formation (Wessels and Markwald, 2000; Jiao et al., 2003). However, there is a debate as to whether Bmp4 is an upstream regulator of *has2* expression. Using explant cultures it has been shown that inhibition of BMP signaling does not affect *has2* expression (Klewer et al., 2006). By contrast, *tbx2* overexpression studies suggested that *has2* expression is controlled by BMP-Smad signaling during cushion formation (Shirai et al., 2009). To determine whether BMP signaling acts downstream of Npnt we inhibited BMP signaling in *npnt* morphants with dorsomorphin,

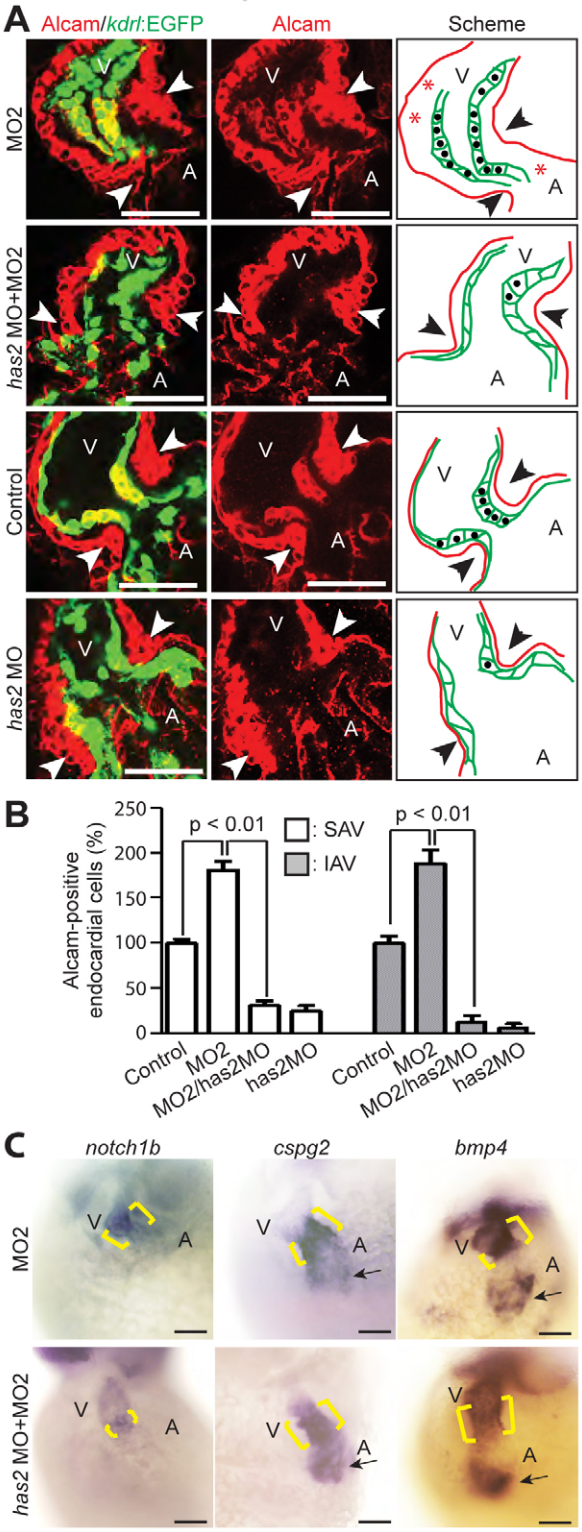

Fig. 6. Has2 knockdown rescues the endocardial phenotype in *npnt* morphants. (**A**) Confocal sections and schematics of whole-mount Alcam-stained (red, indicating myocardium and differentiated endocardial cells) MO2-injected, *has2* MO + MO2-injected, control-injected and *has2* MO-injected embryos from transgenic *Tg(kdrl:EGFP)*^{s843} zebrafish at 52 hpf. Red line, myocardium; green, endocardial cells; black dots, Alcam-positive endocardial cells. Npnt depletion caused an increase in differentiated AV endocardial cells (cuboidal in shape, Alcam positive and EGFP positive) (number of tiers ≥8, SAV; number of tiers ≥5, IAV). Knockdown of Has2 in *npnt* morphants or wild-type embryos reduced the number of tiers to two or fewer in SAV or IAV. Arrowheads indicate the AV boundary. (**B**) Quantitative analysis. Has2 knockdown in *npnt* morphants rescued the AV canal endocardium extension (mean ± s.e.m.). SAV, superior AV; IAV, inferior AV. (**C**) Bright-field images of 52 hpf MO2-injected and *has2* MO + MO2-injected embryos after whole-mount in situ hybridization for *notch1b*, *cspg2* and *bmp4* expression (brackets). Note that Has2 knockdown reduced the expanded expression of *notch1b* but not of *cspg2* or *bmp4* in *npnt* morphants (arrows). A, atrium; V, ventricle. Scale bars: 50 μm.

a chemical antagonist of BMP receptors (Yu et al., 2008), at 25 hpf (see Fig. S7B,C in the supplementary material), and analyzed the embryos at 52 hpf.

Dorsomorphin treatment in *npnt* morphants reduced the number of Alcam-positive AV endocardial cells from 163.6±18.2% (8-10 tiers, SAV) or 176.8.2±17.3% (5-8 tiers, IAV) to 127.3±12.9% (6-8 tiers, SAV) or 107.4±17.3% (3-4 tiers, IAV) compared with wild-type embryos (Fig. 7A,B) and rescued the expanded expression of *notch1b* (Fig. 7C). In wild-type embryos, inhibition of BMP signaling had no effect on the number of Alcam-positive cells (see Fig. S7D in the supplementary material) or upon *notch1b* expression (see Fig. S7E in the supplementary material).

To assess whether ectopic expression of *has2* and *cspg2* is dependent on BMP signaling, we performed in situ hybridization analyses on 52 hpf dorsomorphin-treated *npnt* morphants and wild-type embryos. Dorsomorphin partially rescued the expanded expression of *has2* and *cspg2* at the AV region in *npnt* morphants and abolished ectopic expression of *cspg2* in the inflow tract (Fig. 7C). Expression in wild-type embryos was unaffected (see Fig. S7E in the supplementary material).

To better understand Bmp4-Smad1/5/8 signaling in the AV canal of zebrafish we analyzed the cellular origin of *bmp4* expression and Smad1/5/8 phosphorylation at 52 hpf. Thin sections of wild-type and *npnt* morphant hearts demonstrated that *bmp4* is expressed in the myocardium of the AV canal (see Fig. S7F in the supplementary material). Phosphorylated Smad1/5/8 (p-Smad1/5/8) could be detected in the myocardium and at very low levels in the endocardium (see Fig. S7G,H in the supplementary material). This suggests that myocardial Bmp4 can diffuse in a controlled manner to the AV endocardium, activating p-Smad1/5/8 signaling. By contrast, the level of p-Smad1/5/8 was increased in the expanded AV endocardium of *npnt* morphants to similar levels as in the myocardium (see Fig. S7G,H in the supplementary material).

Thus, our data indicate that knockdown of Npnt causes expanded expression of *bmp4*, which is mainly responsible for the phenotype of *npnt* morphants, and suggest that BMP signaling is an upstream regulator of *has2* and *cspg2* in zebrafish heart (Fig. 7D). Based on our data, we suggest two models. First, Npnt binds to a receptor that is expressed in the chamber myocardium and that this mediates the repression of *bmp4* expression (Fig. 7D, model 1). Second, Npnt regulates the diffusion of Bmp4, preventing paracrine signaling towards the endocardium and the chambers (Fig. 7D, model 2).

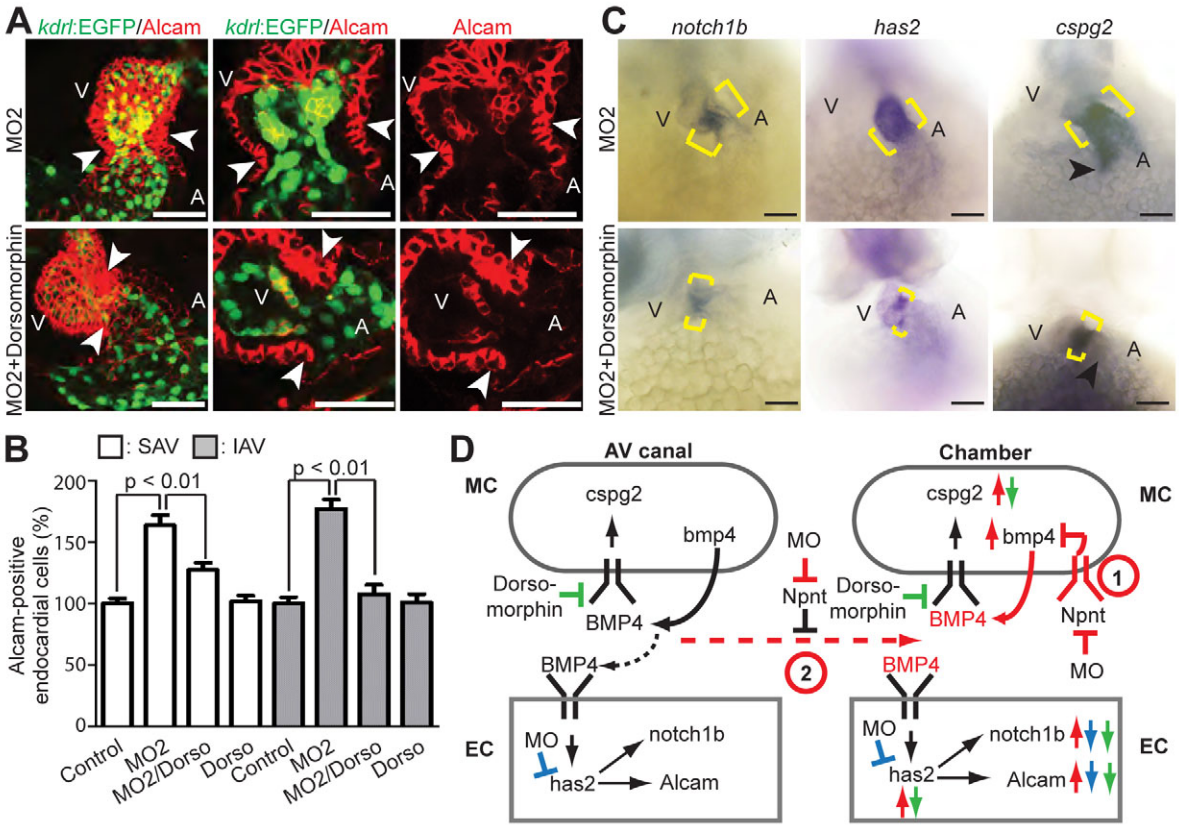

Fig. 7. Inhibition of BMP signaling reduces AV canal expansion. (**A**) Projections of confocal images and confocal sections of hearts of MO2-injected *Tg(kdrl:EGFP)*^{s843} zebrafish embryos at 52 hpf with and without dorsomorphin treatment stained for Alcam (red, indicating myocardium and differentiated endocardial cells). (**B**) Quantitative analysis. Inhibition of BMP signaling by dorsomorphin (Dorso) in the *npnt* morphants rescued the AV canal endocardium extension (mean ± s.e.m.). SAV, superior AV; IAV, inferior AV. (**C**) Bright-field images of 52 hpf untreated and dorsomorphin-treated *npnt* morphants after whole-mount in situ hybridization for *notch1b*, *cspg2* and *has2* expression. Dorsomorphin treatment reduced the expression of *notch1b* and *has2* at the AV boundary in *npnt* morphants (brackets). Moreover, ectopic expression of *cspg2* at the inflow tract in *npnt* morphants is abolished (arrowheads) and *cspg2* expression at the AV boundary is partially rescued. (**D**) Model of the regulatory role of Npnt. 1 and 2 are two possible mechanisms of how Npnt affects Bmp4 signaling. (1) Npnt activates a receptor that is expressed in the chamber myocardium to repress Bmp4 signaling. (2) Npnt inhibits diffusion of Bmp4, resulting in autocrine signaling. Arrows indicate changes after Npnt depletion in wild type (red) or upon *has2* depletion (blue) or dorsomorphin treatment (green) in *npnt* morphants. Red dashed arrow indicates Bmp4 diffusion in the *npnt* morphant. Black dashed arrow indicates controlled Bmp4 diffusion in the wild type. A, atrium; V, ventricle; EC, endocardium; MC, myocardium; MO, morpholino. Scale bars: 50 μm.

DISCUSSION

Our data identify Npnt as a novel regulator of early heart development. Several lines of evidence support this conclusion. First, Npnt knockdown causes 89±7.9% lethality. Second, *npnt* morphant hearts were characterized by an expanded AV canal, increased cardiac jelly, impaired trabeculation and a failure of proper AV valve formation. Third, Has2 knockdown rescued the endocardial phenotype in *npnt* morphants. Fourth, chemical inhibition of BMP signaling rescued AV canal extension in *npnt* morphants. In summary, our data indicate that Npnt regulates the differentiation of the AV segment via Bmp4-Has2 signaling.

It has been shown that regionally specific interactions of myocardium and endocardium are required to initiate the formation of prevalvular mesenchyme (Krug et al., 1985; Mjaatvedt et al., 1987; Wagner and Siddiqui, 2007). Changes in the composition or amount of the ECM can interfere with valve formation. Knockdown of Cspg2 or Has2 results in reduced amounts of cardiac jelly (Mjaatvedt et al., 1998; Camenisch et al., 2000) and in a failure of endocardial cushion formation. By contrast, knockdown of the ECM protein Npnt caused an increase in cardiac jelly. Moreover, it resulted in an extended AV canal on the morphological, cellular and molecular level. This suggests that Npnt does not simply act as a structural protein but functions as a negative regulator of genes involved in AV canal differentiation.

Our data indicate that Npnt is required to maintain the restricted expression of Bmp4 and that expanded *bmp4* expression in *npnt* morphants causes increased expression of *cspg2* and *has2*, which explains the increase in cardiac jelly. *has2* plays an essential role in the formation of cardiac jelly and in the transformation of epithelium to mesenchyme (Camenisch et al., 2000). Has2 knockdown in *npnt* morphants rescued the endocardial phenotype and demonstrates that Npnt controls AV endocardial cell differentiation by regulating *has2* expression. Has2 knockdown in *npnt* morphants, however, did not rescue the ectopic expression of *bmp4* or *cspg2*. Thus, it appears that Bmp4 is an upstream regulator of *has2* expression and that the endocardial phenotype is a consequence of ectopic myocardial *bmp4* expression.

BMP signaling has been shown to regulate *has2* expression (Shirai et al., 2009), although the data are controversial (Klewer et al., 2006). Inhibition of BMP signaling in *npnt* morphants fully rescued the endocardial phenotype, partially rescued the AV canal extension and reduced the expression of *has2* and *cspg2*. In wild-type embryos, dorsomorphin did not affect the basal expression of AV canal marker genes. This might be due to the fact that dorsomorphin treatment resulted in only partial inhibition of BMP-Smad signaling and that complete inhibition could not be achieved even at higher dorsomorphin concentrations (see Fig. S7B,C in the supplementary material). Another possible explanation is that endogenous BMP signaling is redundant at the AV canal. Taken together, our data suggest that Npnt is an upstream regulator of BMP signaling. Moreover, these findings indicate that ectopic BMP signaling regulates *has2* and *cspg2* expression.

It has been suggested that AV endocardial differentiation is mediated through Wnt/β-catenin signaling. *npnt* morphants show many similarities to zebrafish *apc* mutants, in which the Wnt signaling pathway is constitutively activated (Hurlstone et al., 2003). Hearts of both appear normal at 36 hpf but subsequently form excessive cardiac jelly. In *apc* mutants, Wnt/β-catenin signaling is active throughout the heart, resulting in expanded *has2* expression from the AV canal throughout the heart at 72 hpf (Hurlstone et al., 2003). However, our analyses indicate that Npnt knockdown does not result in ectopic activation of Wnt/β-catenin signaling at 52 hpf (see Fig. S8 in the supplementary material).

Our data have identified Npnt as a crucial regulator of AV canal differentiation and ECM composition by controlling Bmp4-Has2 signaling. It will be important in the future to determine how Npnt regulates BMP signaling. It is possible that chamber myocardium expresses a receptor for Npnt that represses Bmp4 signaling (Fig. 7D, model 1). It has been shown that Npnt acts during kidney development as a ligand of integrin α8β1, regulating migration (Brandenberger et al., 2001; Sato et al., 2009). However, during the time of *npnt* expression in the zebrafish heart we did not detect integrin α8 (*itga8*) expression in the heart by in situ hybridization, whereas strong expression was detected in other tissues (see Fig. S9 in the supplementary material). This indicates that Npnt does not signal through integrin α8 during zebrafish heart development. Alternatively, Npnt might activate growth factor receptor signaling. It has been suggested that Npnt can induce signaling through its EGF-like repeats, which are required for Npnt-induced osteoblast differentiation (Kahai et al., 2010). Similarly, it has been suggested that the EGF-like repeats of Versican can bind and activate growth factor receptors (Wight, 2002). Thus, it will be important to determine whether Npnt signals through a receptor during heart development. Another possibility is that Npnt modulates the bioavailability of Bmp4 (Fig. 7D, model 2). Npnt might be required to establish an ECM in which Bmp4 can act only in an autocrine fashion. Knockdown of Npnt might therefore enable diffusion of Bmp4, and thus paracrine signaling, towards the endocardium as well as the chambers (Fig. 7D, model 2).

Previously, it has been shown that mouse embryos lacking a functional *Npnt* gene are born at the expected Mendelian frequency but frequently display kidney agenesis or hypoplasia (Linton et al., 2007). In addition, *Npnt* knockout mice exhibit a skin phenotype (Fujiwara et al., 2011). The heart has thus far not been investigated. The fact that the mouse *Npnt* knockout is not embryonic lethal suggests that the regulation of Bmp4 signaling is more stringent in mammals. This assumption is supported by the finding that the *Npnt* family member Egfl6 is upregulated in *Npnt* knockout mice, partially compensating for Npnt (Fujiwara et al., 2011).

In conclusion, Npnt acts as an inhibitor of Bmp4-Has2 signaling to restrict AV canal differentiation and cardiac jelly swelling in zebrafish. Interference with this pathway results in an expanded AV canal, excessive cardiac jelly and a failure of valve formation.

Acknowledgements
We thank Monika Müller-Boche for excellent fish care; Ingrid Hauck-Schmalenberger and Riad Haceni for technical support; Günes Özhan-Kizil for help with Wnt/β-catenin experiments; Jeroen Bakkers for in situ constructs (*tbx2*, *has2*) and *has2* morpholino; Gillbert Weidinger for the GFP in situ construct, *Tg(TOP:GFP)*^{w25} and *Tg(hsp70l:dkk1-GFP)*^{w32} fish lines; and Didier Stainier for all other in situ constructs. The monoclonal antibodies developed by F. E. Stockdale (s46) and B. Trevarrow (zn8) were obtained from the Developmental Studies Hybridoma Bank (DSHB) developed under the auspices of the NICHD and maintained by The University of Iowa, Department of Biology, Iowa City, IA 52242, USA.

Funding
This work was supported by the Alexander von Humboldt Foundation (Sofja Kovalevskaja Award to F.B.E.), the European Science Foundation (Exchange Grant to F.F.), the International Research Training Group 1566 (PROMISE, DFG) and the Excellence Cluster Cardio-Pulmonary System (DFG). Deposited in PMC for immediate release.

Competing interests statement
The authors declare no competing financial interests.

Supplementary material
Supplementary material for this article is available at
http://dev.biologists.org/lookup/suppl/doi:10.1242/dev.067454/-/DC1

References

Armstrong, E. J. and Bischoff, J. (2004). Heart valve development: endothelial cell signaling and differentiation. *Circ. Res.* **95**, 459-470.
Bakkers, J., Kramer, C., Pothof, J., Quaedvlieg, N. E., Spaink, H. P. and Hammerschmidt, M. (2004). Has2 is required upstream of Rac1 to govern dorsal migration of lateral cells during zebrafish gastrulation. *Development* **131**, 525-537.
Beis, D., Bartman, T., Jin, S. W., Scott, I. C., D'Amico, L. A., Ober, E. A., Verkade, H., Frantsve, J., Field, H. A., Wehman, A. et al. (2005). Genetic and cellular analyses of zebrafish atrioventricular cushion and valve development. *Development* **132**, 4193-4204.
Berdougo, E., Coleman, H., Lee, D. H., Stainier, D. Y. and Yelon, D. (2003). Mutation of weak atrium/atrial myosin heavy chain disrupts atrial function and influences ventricular morphogenesis in zebrafish. *Development* **130**, 6121-6129.
Brandenberger, R., Schmidt, A., Linton, J., Wang, D., Backus, C., Denda, S., Muller, U. and Reichardt, L. F. (2001). Identification and characterization of a novel extracellular matrix protein nephronectin that is associated with integrin alpha8beta1 in the embryonic kidney. *J. Cell Biol.* **154**, 447-458.
Camenisch, T. D., Spicer, A. P., Brehm-Gibson, T., Biesterfeldt, J., Augustine, M. L., Calabro, A., Jr, Kubalak, S., Klewer, S. E. and McDonald, J. A. (2000). Disruption of hyaluronan synthase-2 abrogates normal cardiac morphogenesis and hyaluronan-mediated transformation of epithelium to mesenchyme. *J. Clin. Invest.* **106**, 349-360.
Chi, N. C., Shaw, R. M., De Val, S., Kang, G., Jan, L. Y., Black, B. L. and Stainier, D. Y. (2008). Foxn4 directly regulates tbx2b expression and atrioventricular canal formation. *Genes Dev.* **22**, 734-739.
D'Amico, L., Scott, I. C., Jungblut, B. and Stainier, D. Y. (2007). A mutation in zebrafish hmgcr1b reveals a role for isoprenoids in vertebrate heart-tube formation. *Curr. Biol.* **17**, 252-259.
Dong, P. D., Munson, C. A., Norton, W., Crosnier, C., Pan, X., Gong, Z., Neumann, C. J. and Stainier, D. Y. (2007). Fgf10 regulates hepatopancreatic ductal system patterning and differentiation. *Nat. Genet.* **39**, 397-402.
Dorsky, R. I., Sheldahl, L. C. and Moon, R. T. (2002). A transgenic Lef1/beta-catenin-dependent reporter is expressed in spatially restricted domains throughout zebrafish development. *Dev. Biol.* **241**, 229-237.
Fang, L., Kahai, S., Yang, W., He, C., Seth, A., Peng, C. and Yang, B. B. (2010). Transforming growth factor-beta inhibits nephronectin-induced osteoblast differentiation. *FEBS Lett.* **584**, 2877-2882.
Fujiwara, H., Ferreira, M., Donati, G., Marciano, D. K., Linton, J. M., Sato, Y., Hartner, A., Sekiguchi, K., Reichardt, L. F. and Watt, F. M. (2011). The

basement membrane of hair follicle stem cells is a muscle cell niche. *Cell* **144**, 577-589.
Gaussin, V., Van de Putte, T., Mishina, Y., Hanks, M. C., Zwijsen, A., Huylebroeck, D., Behringer, R. R. and Schneider, M. D. (2002). Endocardial cushion and myocardial defects after cardiac myocyte-specific conditional deletion of the bone morphogenetic protein receptor ALK3. *Proc. Natl. Acad. Sci. USA* **99**, 2878-2883.
Holtzman, N. G., Schoenebeck, J. J., Tsai, H. J. and Yelon, D. (2007). Endocardium is necessary for cardiomyocyte movement during heart tube assembly. *Development* **134**, 2379-2386.
Hsieh, P. C. H., Davis, M. E., Lisowski, L. K. and Lee, R. T. (2006). Endothelial-cardiomyocyte interactions in cardiac development and repair. *Annu. Rev. Physiol.* **68**, 51-66.
Hurlstone, A. F., Haramis, A. P., Wienholds, E., Begthel, H., Korving, J., Van Eeden, F., Cuppen, E., Zivkovic, D., Plasterk, R. H. and Clevers, H. (2003). The Wnt/beta-catenin pathway regulates cardiac valve formation. *Nature* **425**, 633-637.
Jiao, K., Kulessa, H., Tompkins, K., Zhou, Y., Batts, L., Baldwin, H. S. and Hogan, B. L. (2003). An essential role of Bmp4 in the atrioventricular septation of the mouse heart. *Genes Dev.* **17**, 2362-2367.
Jin, S. W., Beis, D., Mitchell, T., Chen, J. N. and Stainier, D. Y. (2005). Cellular and molecular analyses of vascular tube and lumen formation in zebrafish. *Development* **132**, 5199-5209.
Kahai, S., Lee, S. C., Seth, A. and Yang, B. B. (2010). Nephronectin promotes osteoblast differentiation via the epidermal growth factor-like repeats. *FEBS Lett.* **584**, 233-238.
Klewer, S. E., Yatskievych, T., Pogreba, K., Stevens, M. V., Antin, P. B. and Camenisch, T. D. (2006). Has2 expression in heart forming regions is independent of BMP signaling. *Gene Expr. Patterns* **6**, 462-470.
Krug, E. L., Runyan, R. B. and Markwald, R. R. (1985). Protein extracts from early embryonic hearts initiate cardiac endothelial cytodifferentiation. *Dev. Biol.* **112**, 414-426.
Kuphal, S., Wallner, S. and Bosserhoff, A. K. (2008). Loss of nephronectin promotes tumor progression in malignant melanoma. *Cancer Sci.* **99**, 229-233.
Linton, J. M., Martin, G. R. and Reichardt, L. F. (2007). The ECM protein nephronectin promotes kidney development via integrin alpha8beta1-mediated stimulation of Gdnf expression. *Development* **134**, 2501-2509.
Loffredo, C. A. (2000). Epidemiology of cardiovascular malformations: prevalence and risk factors. *Am. J. Med. Genet.* **97**, 319-325.
Mably, J. D., Mohideen, M. A., Burns, C. G., Chen, J. N. and Fishman, M. C. (2003). heart of glass regulates the concentric growth of the heart in zebrafish. *Curr. Biol.* **13**, 2138-2147.
Mjaatvedt, C. H., Lepera, R. C. and Markwald, R. R. (1987). Myocardial specificity for initiating endothelial-mesenchymal cell transition in embryonic chick heart correlates with a particulate distribution of fibronectin. *Dev. Biol.* **119**, 59-67.
Mjaatvedt, C. H., Yamamura, H., Capehart, A. A., Turner, D. and Markwald, R. R. (1998). The Cspg2 gene, disrupted in the hdf mutant, is required for right cardiac chamber and endocardial cushion formation. *Dev. Biol.* **202**, 56-66.
Moorman, A. F. and Christoffels, V. M. (2003). Cardiac chamber formation: development, genes, and evolution. *Physiol. Rev.* **83**, 1223-1267.
Okagawa, H., Nakagawa, M. and Shimada, M. (1996). Immunolocalization of vinculin in the heart of the early developing rat embryo. *Anat. Rec.* **245**, 699-707.
Sato, Y., Uemura, T., Morimitsu, K., Sato-Nishiuchi, R., Manabe, R., Takagi, J., Yamada, M. and Sekiguchi, K. (2009). Molecular basis of the recognition of nephronectin by integrin alpha8beta1. *J. Biol. Chem.* **284**, 14524-14536.
Shirai, M., Imanaka-Yoshida, K., Schneider, M. D., Schwartz, R. J. and Morisaki, T. (2009). T-box 2, a mediator of Bmp-Smad signaling, induced hyaluronan synthase 2 and Tgfbeta2 expression and endocardial cushion formation. *Proc. Natl. Acad. Sci. USA* **106**, 18604-18609.
Smith, K. A., Joziasse, I. C., Chocron, S., van Dinther, M., Guryev, V., Verhoeven, M. C., Rehmann, H., van der Smagt, J. J., Doevendans, P. A., Cuppen, E. et al. (2009). Dominant-negative ALK2 allele associates with congenital heart defects. *Circulation* **119**, 3062-3069.
Srivastava, D. (2006). Making or breaking the heart: from lineage determination to morphogenesis. *Cell* **126**, 1037-1048.
Stainier, D. Y. (2001). Zebrafish genetics and vertebrate heart formation. *Nat. Rev. Genet.* **2**, 39-48.
Wagner, M. and Siddiqui, M. A. (2007). Signal transduction in early heart development (I): cardiogenic induction and heart tube formation. *Exp. Biol. Med.* **232**, 852-865.
Walsh, E. C. and Stainier, D. Y. (2001). UDP-glucose dehydrogenase required for cardiac valve formation in zebrafish. *Science* **293**, 1670-1673.
Wessels, A. and Markwald, R. (2000). Cardiac morphogenesis and dysmorphogenesis. I. Normal development. *Methods Mol. Biol.* **136**, 239-259.
Westerfield, M. (1993). *The Zebrafish Book: a Guide for the Laboratory Use of Zebrafish (Brachydanio rerio)*. Eugene, OR: University of Oregon Press.
Wight, T. N. (2002). Versican: a versatile extracellular matrix proteoglycan in cell biology. *Curr. Opin. Cell Biol.* **14**, 617-623.
Yelon, D. (2001). Cardiac patterning and morphogenesis in zebrafish. *Dev. Dyn.* **222**, 552-563.
Yelon, D., Horne, S. A. and Stainier, D. Y. (1999). Restricted expression of cardiac myosin genes reveals regulated aspects of heart tube assembly in zebrafish. *Dev. Biol.* **214**, 23-37.
Yu, P. B., Hong, C. C., Sachidanandan, C., Babitt, J. L., Deng, D. Y., Hoyng, S. A., Lin, H. Y., Bloch, K. D. and Peterson, R. T. (2008). Dorsomorphin inhibits BMP signals required for embryogenesis and iron metabolism. *Nat. Chem. Biol.* **4**, 33-41.
Zang, H. Y., Lardelli, M. and Ekblom, P. (1997). Sequence of zebrafish fibulin-1 and its expression in developing heart and other embryonic organs. *Dev. Genes Evol.* **207**, 340-351.

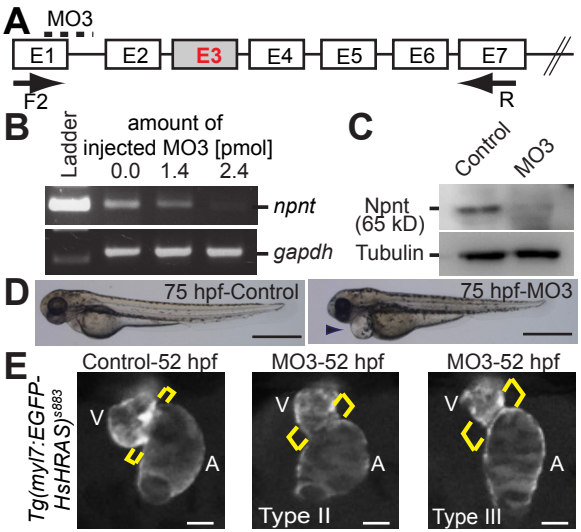
A
MO3
E1
E2
E3
E4
E5
E6
E7
F2
R
B
Ladder
amount of injected MO3 [pmol]
0.0 1.4 2.4
npnt
gapdh
C
Control
MO3
Npnt (65 kD)
Tubulin
D
75 hpf-Control
75 hpf-MO3
E
Control-52 hpf
MO3-52 hpf
MO3-52 hpf
Tg(myl7:EGFP-HsHRAS)s883
V
A
Type II
Type III

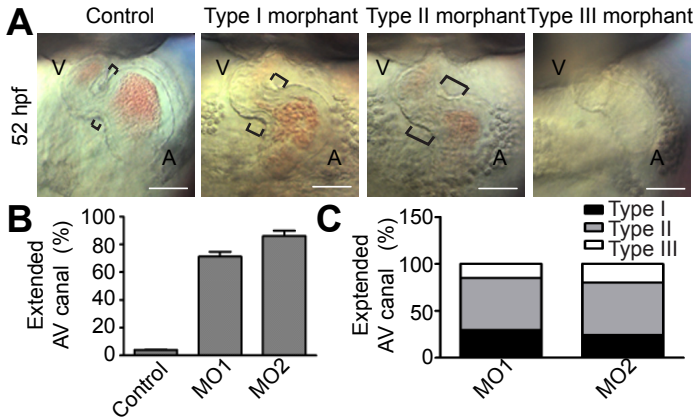
A
Control
Type I morphant
Type II morphant
Type III morphant
52 hpf
V
A
B
Extended AV canal (%)
100
80
60
40
20
0
Control
MO1
MO2
C
Exptended AV canal (%)
150
100
50
0
Type I
Type II
Type III
MO1
MO2


E1 TTCGAGTCTGACCACTGACGGATTTAAATCTCATCATCATTCCCATTCACAGACCGGACACCAGCCGCGACGTCTGGATAATA
E1 TTCGAGTCTGACCACTGACGGATTTAAATCTCATCATCATTCCCATTCACAGACCGGACACCAGCCGCGACGTCTGGATAATA
CGCGCAGTGCACGCGCGCGGAGATGTGGATCATAAAGTTCATGTTGATGTGGACCTGCTGGATCGCAGTGGACGCGGACTTCGATG
CGCGCAGTGCACGCGCGCGGAGATGTGGATCATAAAGTTCATGTTGATGTGGACCTGCTGGATCGCAGTGGACGCGGACTTCGATG
GCAGGTG E2 E3 ---------- E4 E5 E6 E7 E8 E9
GCAGGTG E2 E3 CCTCTACGTCTTAACCCGCAGAGTAATCGGGATAAGGTGTCAGCCCCAAG E4 E5 E6 E7 E8 E9
E10 E11 E12 E13 GATCGTGAAGGGCGAGCGGCGGAGAGGCCGCAAGGGCGAAATTGCTCTGGATGACATGAGTCTCAAAC
E10 E11 E12 E13 GATCGTGAAGGGCGAGCGGCGGAGAGGCCGCAAGGGCGAAATTGCTCTGGATGACATGAGTCTCAAAC
GAG---------- E14 AGGATTCGAGAAAGATGGACACCTTATGGAAAGGGACGTG
GAGGTTCCTGTCAGGAAGAGCACAATCTGAGGAGACTTTAA E14 ----------
GCCTTCTGTCAGTCCCGATATGGTAATGGTGCACTTTCTCAGCGGCTGCAAGTGCATGTCCCAGCTCAACAGAGTGCGGTAGGA

TGACGTATTTTTGTAGAACAAACAGGGAAAGTATTTTAGTACTTCAGATTGTATCGTCTCTAAGTCAGTATTGTAGTTTTTTCAAT

GGGTTGAAGTTGATCAGTATTTTTCATAAGGAATTGGTTGCTAAAAC

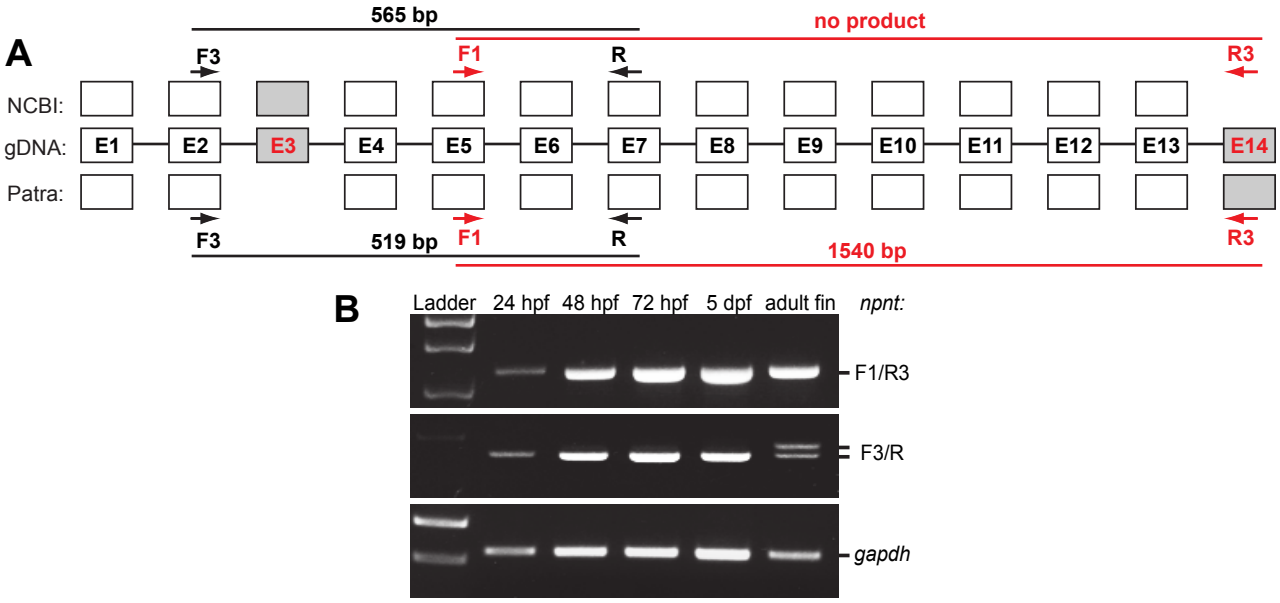

C

```
NCBI   1    MWIIKFMLMWTCWIAVDADFDGRWSRQMSSSNGLCRYGGRIDCCWGWTRVSWGQCQPLYVLTRRVIGIRC  70
            MWIIKFMLMWTCWIAVDADFDGRWSRQMSSSNGLCRYGGRIDCCWGWTRVSWGQCQPL
Patra  1    MWIIKFMLMWTCWIAVDADFDGRWSRQMSSSNGLCRYGGRIDCCWGWTRVSWGQCQPL------------  68
                                EGF-like domain          EGF_CA          EGF-like domain
NCBI   71   QPQALCQHGCKHGECVGPNKCKCHPGYTGKTCNQDLNECGLKPRPCKHRCMNTFGSFKCYCLNGFMLLPD 140
                 CQHGCKHGECVGPNKCKCHPGYTGKTCNQDLNECGLKPRPCKHRCMNTFGSFKCYCLNGFMLLPD
Patra  99   -----CQHGCKHGECVGPNKCKCHPGYTGKTCNQDLNECGLKPRPCKHRCMNTFGSFKCYCLNGFMLLPD 123
                                                                  EGF_CA
NCBI   141  GSCANARTCSMANCQYGCEVMKGEVRCQCPSPGLQLAPDGRTCVDVDECAAGLAVCPRFRKCINTFGSYI 210
            GSCANARTCSMANCQYGCEVMKGEVRCQCPSPGLQLAPDGRTCVDVDECAAGLAVCPRFRKCINTFGSYI
Patra  124  GSCANARTCSMANCQYGCEVMKGEVRCQCPSPGLQLAPDGRTCVDVDECAAGLAVCPRFRKCINTFGSYI 193
                                       EGF_CA
NCBI   211  CKCHDGFDLQYVNGKYQCTDVNECSLGQHQCGPYATCYNTPGSYKCKCKEDYRGVGYDCKPIPKVVIDPP 280
            CKCHDGFDLQYVNGKYQCTDVNECSLGQHQCGPYATCYNTPGSYKCKCKEDYRGVGYDCKPIPKVVIDPP
Patra  194  CKCHDGFDLQYVNGKYQCTDVNECSLGQHQCGPYATCYNTPGSYKCKCKEDYRGVGYDCKPIPKVVIDPP 263

NCBI   281  RPGKTTPSSNNNKGGNKIPGSDQKRTTTTVRPPVTAKRISPTITTTTTTTKPPPTKKITPPARVPVTTTR 350
            RPGKTTPSSNNNKGGNKIPGSDQKRTTTTVRPPVTAKRISPTITTTTTTTKPPPTKKITPPARVPVTTTR
Patra  264  RPGKTTPSSNNNKGGNKIPGSDQKRTTTTVRPPVTAKRISPTITTTTTTTKPPPTKKITPPARVPVTTTR 333
                                                                  RGD domain
NCBI   351  KPFIPTRKPPVLVTTKPKVPTHQHTTTKVPVVTAVVPFIPTRRPFTIPFVTPIDNSIKDITQKQRGDVHI 420
            KPFIPTRKPPVLVTTKPKVPTHQHTTTKVPVVTAVVPFIPTRRPFTIPFVTPIDNSIKDITQKQRGDVHI
Patra  334  KPFIPTRKPPVLVTTKPKVPTHQHTTTKVPVVTAVVPFIPTRRPFTIPFVTPIDNSIKDITQKQRGDVHI 403
                                                        MAM domain
NCBI   421  PRNHGKNNVLGIDLDIELGNTEEELKDDPESGYLSCSFDHGLCGWIQRREGDLHWETSEDPSGGRYLTIS 490
            PRNHGKNNVLGIDLDIELGNTEEELKDDPESGYLSCSFDHGLCGWIQRREGDLHWETSEDPSGGRYLTIS
Patra  404  PRNHGKNNVLGIDLDIELGNTEEELKDDPESGYLSCSFDHGLCGWIQRREGDLHWETSEDPSGGRYLTIS 473

NCBI   491  EGGEKRGGRGAQLILPLKTPWNEGNLCLAFRHNMAGHHVGMLQVFVQKGRQHSPAVWGRTGGNGWRSTQI 560
            EGGEKRGGRGAQLILPLKTPWNEGNLCLAFRHNMAGHHVGMLQVFVQKGRQHSPAVWGRTGGNGWRSTQI
Patra  474  EGGEKRGGRGAQLILPLKTPWNEGNLCLAFRHNMAGHHVGMLQVFVQKGRQHSPAVWGRTGGNGWRSTQI 543

NCBI   561  TLWGNGLESVIVKGERRRGRKGEIALDDMSLKRGSCQEEHNLRRL 605
            TLWGNGLESVIVKGERRRGRKGEIALDDMSLKR   ++    L
Patra  544  TLWGNGLESVIVKGERRRGRKGEIALDDMSLKREDSRKMDTLWKGTWPSVSPDMVMVHFLSGCKCMSQLNRVR 616
```

D

Motif Scan results:

List of matches

```
ASX_HYDROXYL: 120-131, 202-213, 247-258
CYS_RICH:      70-258
EGF_1:         91-102
EGF_2:         91-102, 129-143
EGF_CA:       105-129, 185-211, 230-256
EGF_3:         66-103, 105-144, 185-223,
              230-270
MAM_2:        454-598
PRO_RICH:     332-402
THR-RICH:     306-377
```

Frequent patterns:

```
AMIDATION:          578-581
C_tripleX:           71- 87
CAMP_PHOSPHO_SITE: 304-307, 317-320, 336-339, 592-595
CK2_PHOSPHO_SITE:  182-185, 401-404, 406-409, 441-444,
                   477-480, 488-491, 595-598
EGF_alliinase:      90-109
MYRISTYL:           79- 84, 125-130, 141-146, 207-212,
                   237-242, 252-257, 497-502
PKC_PHOSPHO_SITE:   62- 64,  98-100, 126-128, 253-255, 309-311, 315-317,
                   329-331, 335-337, 348-350, 356-358, 364-366, 376-378,
                   391-393, 406-408, 411-413, 590-592
RGD:               415-417          TIL:               166-189
Transglut_C:       519-538          TYR_PHOSPHO_SITE:  446-453
```

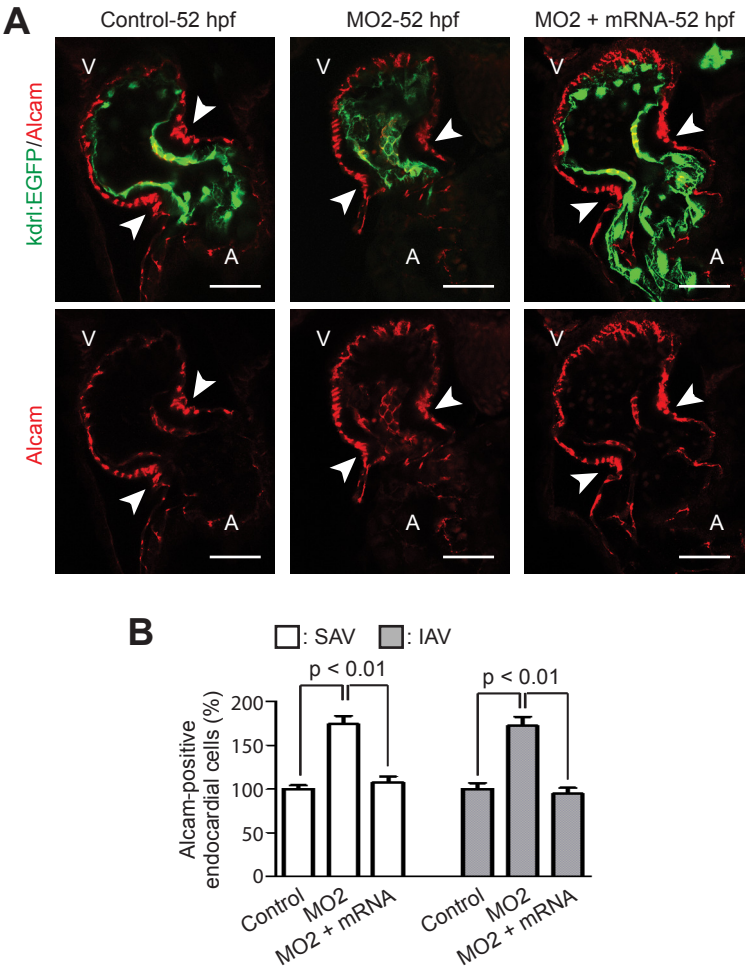
A
Control-52 hpf
MO2-52 hpf
MO2 + mRNA-52 hpf
kdrl:EGFP/Alcam
Alcam
V
A
B
: SAV
: IAV
p < 0.01
p < 0.01
Alcam-positive endocardial cells (%)
200
150
100
50
0
Control
MO2
MO2 + mRNA
Control
MO2
MO2 + mRNA
C
Control-52 hpf
MO2-52 hpf
MO2 + mRNA-52 hpf
bmp4
cspg2
V
A

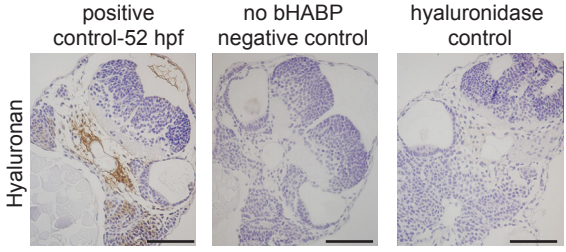
positive
control-52 hpf
no bHABP
negative control
hyaluronidase
control
Hyaluronan

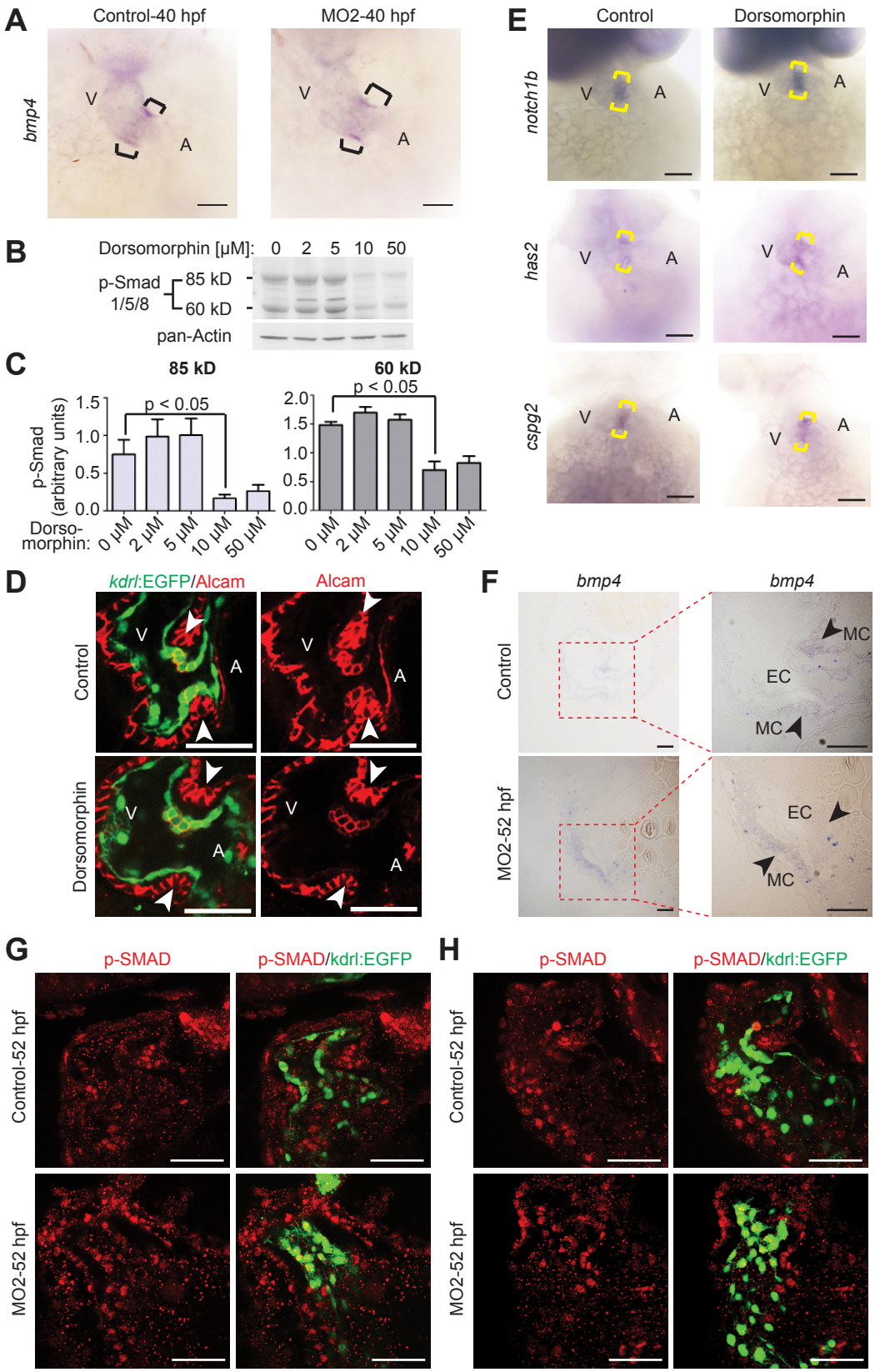
A
Control-40 hpf
MO2-40 hpf
bmp4
V
A
B
Dorsomorphin [μM]: 0 2 5 10 50
p-Smad 1/5/8
85 kD
60 kD
pan-Actin
C
85 kD
60 kD
p < 0.05
p < 0.05
p-Smad (arbitrary units)
Dorso-morphin:
0 μM
2 μM
5 μM
10 μM
50 μM
D
kdrl:EGFP/Alcam
Alcam
Control
Dorsomorphin
E
Control
Dorsomorphin
notch1b
has2
cspg2
F
bmp4
bmp4
Control
MO2-52 hpf
MC
EC
G
p-SMAD
p-SMAD/kdrl:EGFP
Control-52 hpf
MO2-52 hpf
H
p-SMAD
p-SMAD/kdrl:EGFP
Control-52 hpf
MO2-52 hpf

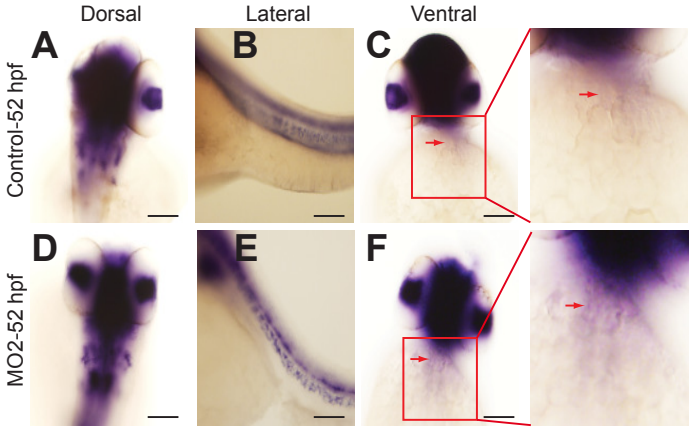
Dorsal
Lateral
Ventral
A
B
C
D
E
F
Control-52 hpf
MO2-52 hpf

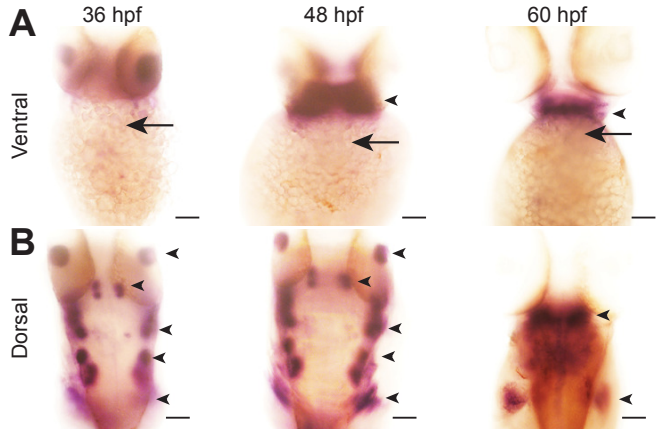

C

UGID:2630752

ID	Name	Species	ID%
NP_001108383.1	LOC100141346	*D. rerio*	100.0
NP_001001309.1	integrin alpha-8 precursor	*M. musculus*	74.7
NP_003629.1	integrin alpha-8 precursor	*H. sapiens*	73.5
NP_001167443.1	integrin alpha-8	*R. norvegicus*	75.3